Journal of Crystallization Process and Technology, **2014, 4, 39-45**
Published Online January 2014 (http://www.scirp.org/journal/jcpt)
http://dx.doi.org/10.4236/jcpt.2014.41006

Single Crystal Growth of Lanthanum(III) Molybdate(VI) ($La_4Mo_7O_{27}$) Using H_3BO_3 Flux

Muthaiyan Rajalakshmi, Ravanan Indirajith, Rengasamy Gopalakrishnan*

Crystal Research Laboratory, Department of Physics, Anna University, Chennai, India.
Email: *krgkrishnan@annauniv.edu, krgkrishnan@yahoo.com

Received February 3rd, 2012; revised August 17th, 2013; accepted August 22nd, 2013

ABSTRACT

Single crystals of $La_4Mo_7O_{27}$ have been successfully grown by the flux growth method H_3BO_3 as the flux in a plantium crucible using the starting materials of La_2O_3, H_3BO_3 and MoO_3 in a molar ratio of 0.16:0.16:0.68, in which H_3BO_3 acted as a flux. Transparent colorless crystals were obtained with size of 0.8 × 0.3 × 0.2 mm^3 under the optimized crystal growth conditions: growth temperature of 727˚C, growth time of 95 h and cooling rate of 0.5˚C/hr. A well-developed morphology of the crystals was observed and analyzed. The preparation process of starting materials on crystal growth was investigated. The grown crystals were characterized by powder X-ray diffraction (PXRD), EDAX, SEM, UV-Vis, photoluminescence studies, thermal analysis, dielectric studies and second harmonic generation (SHG). The results are presented and discussed.

KEYWORDS

Flux Growth; Powder X-Ray Diffraction; $La_4Mo_7O_{27}$; Thermal Analysis; Optical Properties; Second Harmonic Generation (SHG)

1. Introduction

In the past few decades, due to the fast development of the laser technique, nonlinear optical (NLO) crystals have been playing an important role, and have been widely used in high-speed information processing, optical data storage, laser medicine, laser frequency conversion, signal communications, optical modulating, etc. in the expanding field of integrated optics [1-4]. Rare-earth elements have unique characteristics unlike most of other elements on the periodic table. These consist of thirty elements all together separated into two different groups: lanthanides (fifteen total) and actinides (fifteen total). The lanthanides are elements famous for their 4 f shell level that resides deep inside the atom itself. Each lanthanide contains a 4 f orbital shielded by 4 d and 5 p orbital electrons. Electrical, optical, photonic and thermal uses were deduced from research with each rare-earth element. The extensive research for the new rare earth (R) and other element complex borates is of great interest because of their potential applications in nonlinear optics (NLO) and laser engineering. The isoformular compounds $Eu_4Mo_7O_{27}$ [5] and $Gd_4Mo_7O_{27}$ [6] have a similar structure.

The flux growth technique is particularly preferable because it readily allows crystal growth at a temperature well below the melting point of the solute. In addition, crystals grown from flux have an enhedral habit and a reasonably lower degree of dislocation density. In this paper, the flux growth of $La_4Mo_7O_{27}$ single crystals by high temperature solution growth technique (flux growth method) is reported. The structure of $La_4Mo_7O_{27}$ crystal was first described by Benjamin van der Wolf *et al.* [7]. $La_4Mo_7O_{27}$ crystallizes in the orthorhombic system, space group $Pca2_1$, with a = 14.1443 (14) Å, b = 7.2931 (4) Å, c = 22.9916 (13) Å, V = 2371.7 (3) Å^3 and Z = 4. For the growth of crystals by flux method, not only the nature of flux is important, but also the ratio of flux is essential. Many trials were made to obtain a good transparent crystal from flux growth. Nevertheless, this mate-

*Corresponding author.

rial also has some intrinsic weaknesses and it is typically difficult to grow high quality crystals to a size practical for optical applications.

2. Synthesis and Crystal Growth

Crystals of the orthorhombic phase $La_4Mo_7O_{27}$ (lanthanum molybdenum oxide) were obtained from a non-stoichiometric melt in the pseudo-ternary system La_2O_3-MoO_3-B_2O_3. The title compound of $La_4Mo_7O_{27}$ was synthesized using high-temperature solid-state technique. The starting materials were La_2O_3 (99.99%, AlfaAesar), H_3BO_3 (99.8%, Merck) and MoO_3 (99.95%, Himedia) in a molar ratio of 0.16:0.16:0.68. An excess of 0.5 - 0.8 mol H_3BO_3 was added to compensate any loss due to vaporization of H_3BO_3 in the process of high-temperature reaction. The experiments were carried out in a resistance-heated furnace. A controller (Eurotherm, model No. 2704) with an accuracy of ±0.01˚C was used to control the furnace temperature. **Figure 1** shows the schematic setup used for the growth of lanthanum molybdenum oxide single crystals. The furnace was made up of silicon carbide rods and thick ceramic slabs are used as the walls of the furnace.

The starting materials of La_2O_3 (99.99%, AlfaAesar), H_3BO_3 (99.8%, Merck) and MoO_3 (99.95%, Himedia) were mixed in a molar ratio of 0.16:0.16:0.68 in a platinum crucible and preheated at 1023 K for 90 h to decompose the boron acid. After 95 h at this temperature the sample was quenched in air, washed with water at 60˚C. A series of grinding and heating were performed prior to final heating at 827˚C and cooled at rate of 0.5/h to 820˚C and quenched again in air. **Figure 2** shows the temperature profile of the experiment. A further similar heating-cooling cycle yielded colourless crystals of $La_4Mo_7O_{27}$ and they were separated mechanically from the solidified melt. The $La_4Mo_7O_{27}$ crystal was very stable in air and in moist environments, which demonstrated that it is chemically stable and non-hygroscopic. Samples obtained were checked by powder X-ray diffraction analysis to confirm the single-phase of $La_4Mo_7O_{27}$.

Several ratios of La_2O_3:H_3BO_3:MoO_3 were tried for growing $La_4Mo_7O_{27}$ crystals, but the ratio 0.16:0.16:0.68, yielded crystals. **Table 1** shows the experimental summary of the $La_4Mo_7O_{27}$ crystal growth. The present experimental investigation showed that $La_4Mo_7O_{27}$ crystals with good optical quality grown from H_3BO_3 solvent (flux). Transparent, colorless single crystals with dimensions 0.8 × 0.3 × 0.2 mm^3 were obtained. **Figure 3** shows the as grown $La_4Mo_7O_{27}$ crystal from flux growth technique.

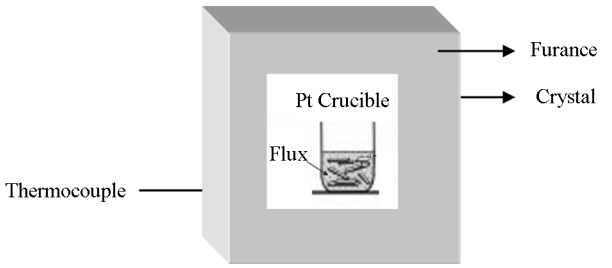

Figure 1. Schematic of furnace setup for the growth of $La_4Mo_7O_{27}$ single crystal by flux growth technique.

3. Results and Discussion

3.1. XRD Analysis

Powder XRD analysis of the $La_4Mo_7O_{27}$ was performed using the desktop Bruker, D2 Phaser Instrument with a diffracted-beamed monochromator set for CuKα (λ = 1.5418 Å) radiation at room temperature in the an gular range of 2θ = 10˚ - 70˚, with a scan step width of 0.01˚, and a fixed counting time of 1 s/step. The obtained powder XRD pattern is shown in **Figure 4**. The experimental Powder XRD pattern of $La_4Mo_7O_{27}$ is in good agreement with the literature data [7].

3.2. EDX Studies

The EDX analysis is a powerful tool in determining the presence of the constituent elements in a given sample. The EDX measurements were made using an INCA 200 energy dispersive X-ray micro-analyzer. **Figure 5(a)** shows surface region of sample for EDX analysis. The red colour square region indicates the experimental portion for EDX. The EDX spectrum is shown in **Figure 5(b)** and the elemental composition is figured in **Table 2**. The presence of the constituent elements (lanthanum, molybdenum and oxygen) of the $La_4Mo_7O_{27}$ crystal was confirmed by the occurrence of their respective peaks. There are no signs for the presence of flux in the crystal. Hence, the formation of "flux-free" $La_4Mo_7O_{27}$ crystal is

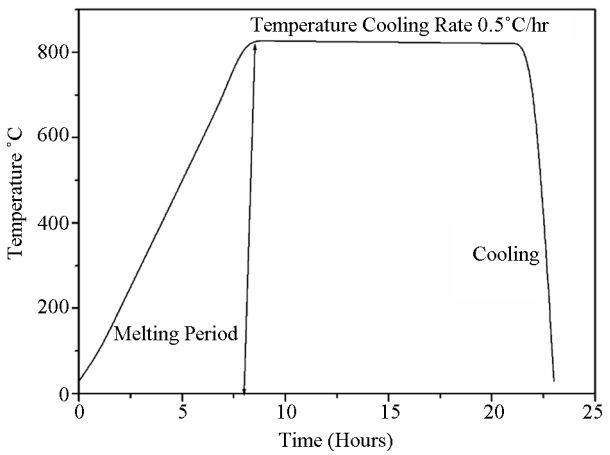

Figure 2. Temperature profile used for the growth of lanthanum molybdenum oxide single crystals.

Table 1. Summary of the crystal growth experiment.

La_2O_3:MoO_3:B_2O_3	Temperature for crystallization (˚C)	Cooling rate (˚C/h)	Size and quality of crystals grown
0.16:0.16:0.68	827	1	Poor
0.16:0.16:0.68	827	0.5	(0.8 × 0.3 × 0.2 mm^3), (0.2× 0.2 × 0.1 mm^3)
0.16:0.16:1	827	0.1	-
0.16:0.2:2	827	0.1	-
0.16:0.2:3	827	0.1	-

Figure 3. As grown $La_4Mo_7O_{27}$ crystal from flux growth technique.

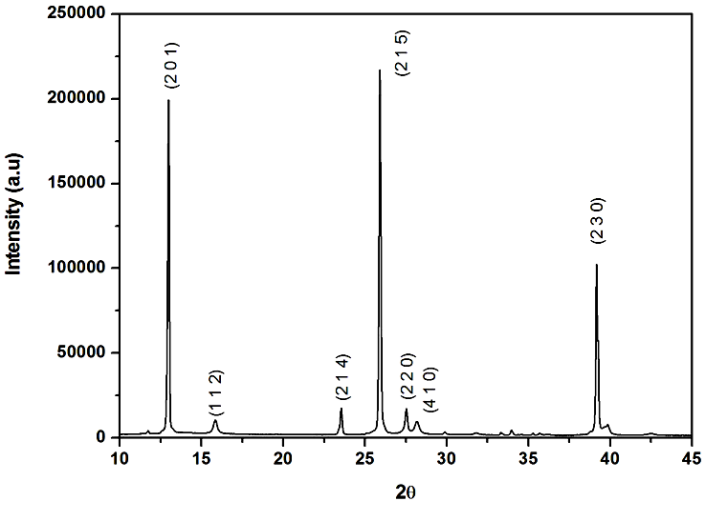

Figure 4. Powder XRD pattern of $La_4Mo_7O_{27}$.

confirmed.

3.3. SEM Studies

The SEM image (Figure 6) shows that the as grown lanthanum molybdenum oxide crystal exhibits uniform hexagonal shape. Most of the crystals were found to have hexagonal plate shape with typical edge angles of 45˚ and with very flat surfaces. The size of the one crystallite is about 3.85 μm length, 472.0 nm in diameter. The smooth surfaces and the sharp edges confirmed that these small single crystals are of high quality. Generally speaking, the growth morphology of a crystal is determined by the relative growth rates of all the possible

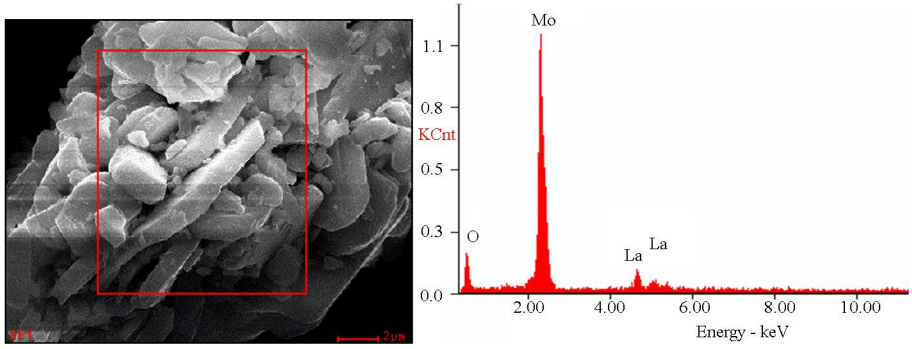

(a) (b)

Figure 5. (a) Surface region of the $La_4Mo_7O_{27}$ crystal; (b) The EDX spectrum of the $La_4Mo_7O_{27}$ crystal.

Table 2. Elemental compostion of the $La_4Mo_7O_{27}$ crystal.

Element	Wt%	At%
Ok	27.97	70.92
MoL	61.49	26.00
LaL	10.54	03.08

faces.

3.4. UV-Vis Studies

The absorption spectrum of lanthanum molybdenum oxide is shown in **Figure 7(a)**. According to the experimental measurements, the crystal has a transparent region in the 455 - 2500 nm range with a cutoff at 455 nm. The absorption decreases rapidly around 450 nm. Therefore, there is little optical absorption in the visible region of the UV-Vis-NIR spectrum. Crystals of lanthanum molybdenum oxide may be useful for applications in the wavelength region of 450 - 2500 nm. At the wavelength, just above 500 nm, there is a sudden increase in absorbance in the crystal due to electronic excitation of lanthanum molybdenum oxide. Since the crystal is possessing delocalized electron cloud for charge transfer, the absorbance is less between 500 and 2000 nm. Hence, the crystal can be used for SHG and optical applications [8].

3.5. Optical Band Gap

Optical band gap of the title compound was calculated from the transmittance spectrum. The measured transmittance (T) was used to calculate the absorption coefficient (α) using the following formula,

$$\alpha = \frac{2.3026 \log\left(\frac{1}{T}\right)}{t} \quad (1)$$

where, t is the thickness of the sample.

The optical band gap (E_g) was evaluated from the transmission spectrum and the optical absorption coefficient (α) near the absorption edge is given by the Tauc's

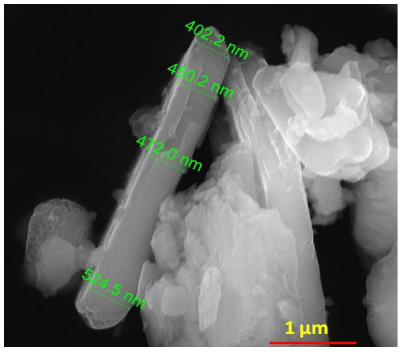

(a)

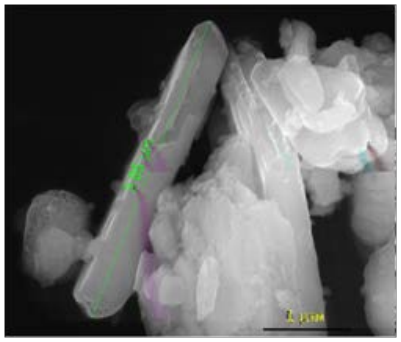

(b)

Figure 6. SEM micrographs of lanthanum molybdenum oxide crystals.

equation [9,10].

$$h\upsilon\alpha = A\left(h\upsilon - E_g\right)^m \quad (2)$$

where, A is a constant, α is the optical absorption coefficient, h is the Planck's constant and ν is the frequency of the incident photon, E_g the optical band gap and m is a constant which characterizes the nature of band transition. Among all possible transitions, m = 1/2 is more suitable for this crystal since it gives the best linear curve in the band edge and hence the transition is direct allowed. The band gap was calculated from the plot between $h\nu$ and $(\alpha h\nu)^{1/2}$ as shown in the **Figure 7(b)**. The optical band gap is found to be 2.6 eV for lanthanum molybdenum

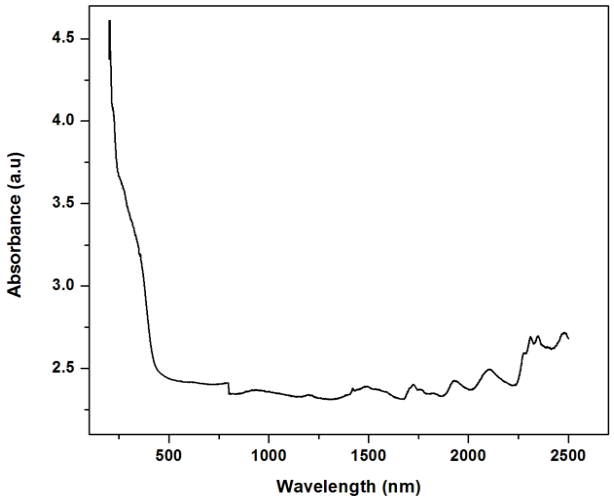

(a)

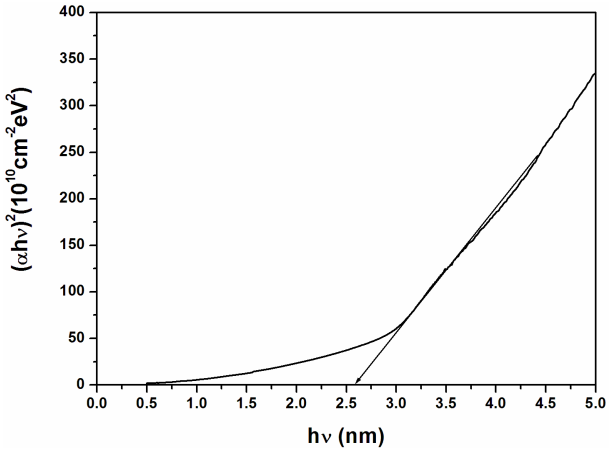

(b)

Figure 7. (a) Absorbance spectrum of the grown lanthanum molybdenum oxide; (b) Plot of photon energy with $(\alpha hv)^{1/2}$ of lanthanum molybdenum oxide.

oxide.

3.6. Photoluminescence (PL) Analysis

Photoluminescence is the process by which a material is bombarded with photons, excited, and then emits photons back. The optical behaviour of the title compound was analysed by PL measurements using HORIBA JOBINYVON Luminescence spectrometer. Argon ion laser was used as an input source with excitation wavelength of 488 nm for present study. The recorded spectrum is shown in **Figure 8**, in which, the maximum intensity is observed around 534 nm. Generally, a green-yellow emission is observed in PL spectra, due to recombination of photo generated holes with singly ionized charge state of specific defect [11]. However, absence of the green yellow emission in the sample indicates the potential of strategy to produce a low concentration of oxygen defects and high optical quality of single crystal $La_4Mo_7O_{27}$

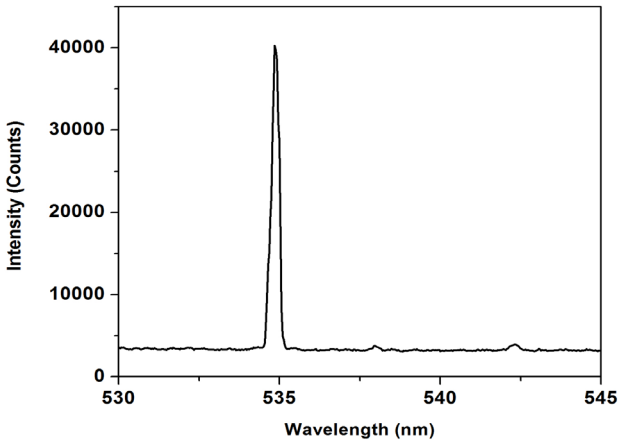

Figure 8. Photoluminescence spectrum of $La_4Mo_7O_{27}$ excited by a 488 nm laser.

[12,13]. The emission of 534 nm could not contribute to the transition from the conduction band to the valence band. The emission does not originate from a transition between the conduction and valence band; it comes from a deep-level or trap-state emission.

3.7. Thermal Analysis

The thermal stability of the crystal is a very important factor for potential application. In order to know the thermal stability of the material, thermogravimetric analysis (TGA) as well as differential thermal analysis (DTA) were carried out on polycrystalline samples of $La_4Mo_7O_{27}$ in flowing N_2 ambient. For this purpose, a NETZSCH STA 409 C/CD simultaneous DT/TG analyser with a heating rate of 2.5 K/min was employed. The TGA thermogram is shown in **Figure 9**. From the figure, it is evident that the compound is stable up to 100˚C and the compound begins to decompose at this temperature. Structural phase transitions occur in the sample and two more endothermic peaks indicate phase transitions at 91.4˚C and 107.2˚C.

3.8. Dielectric Studies

The dielectric study of $La_4Mo_7O_{27}$ was carried out using the instrument, HIOKI 3532-50 LCR HITESTER. The capacitance (C) and quality factor (Q) of the sample at different temperatures and with different frequency were measured. The compound was prepared in pellet form of circular cross section (area ~0.90×10^{-4} m^2 and thickness ~0.30×10^{-2} m) by applying pressure. The pellets were then sintered in air for 12 hrs at 50˚C. The pellet covered with film of silver paint on the opposite surfaces to obtain a good contact was inserted between the two silver electrodes. The dielectric constant (ε') and dielectric loss (ε'') of the sample were calculated using the following equation [14,15].

$$\varepsilon' = \frac{Ct}{\varepsilon_0 A} \quad (3)$$

$$\varepsilon'' = \frac{\varepsilon'}{Q} \quad (4)$$

where C is the capacitance of the capacitor in Farad, d is the thickness, A is the face area of the pellet, ε_0 is the permittivity of free space and Q is the quality factor respectively.

The plots of dielectric constant (ε') and dielectric loss with frequency for various temperatures are shown in **Figures 10(a)** and **(b)**. The dielectric constant is high in the lower frequency region and variation of dielectric constant (ε') with log$f$ decreases with increase in frequency. The very high value of dielectric constant at low frequencies may be due to the presence of all the four components namely, space charge, orientational, electronic and ionic polarisations. The dielectric loss was also studied as a function of frequency for different temperatures and is shown in **Figure 10(b)**. The low dielectric loss at high frequencies for the given sample indi-

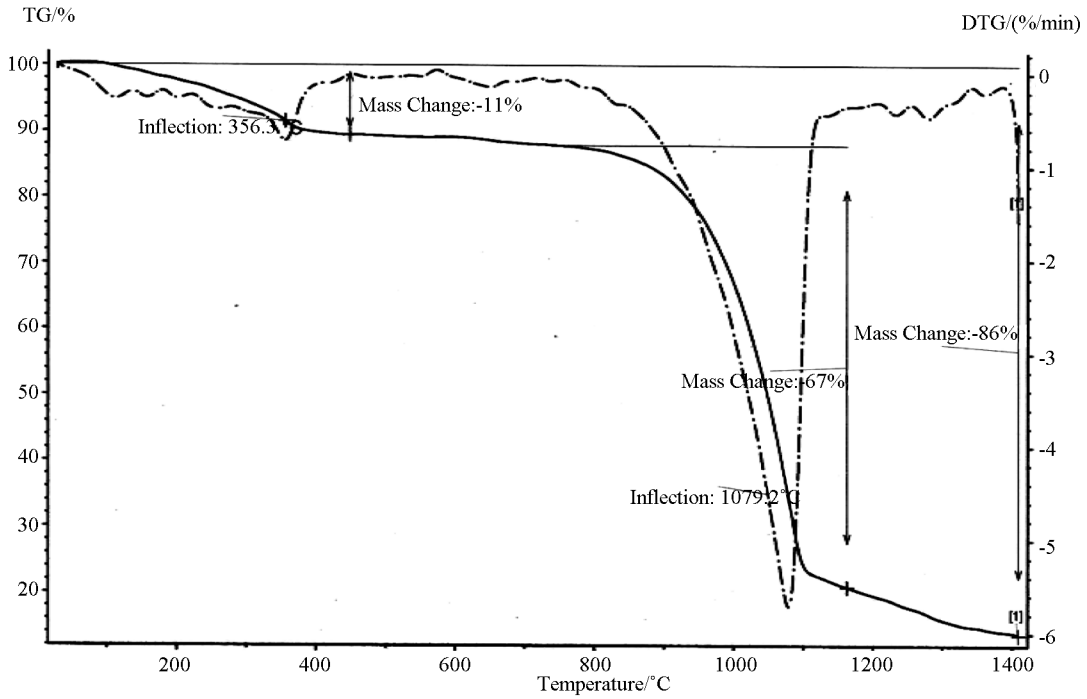

Figure 9. TG/DTaaaG curves of $La_4Mo_7O_{27}$.

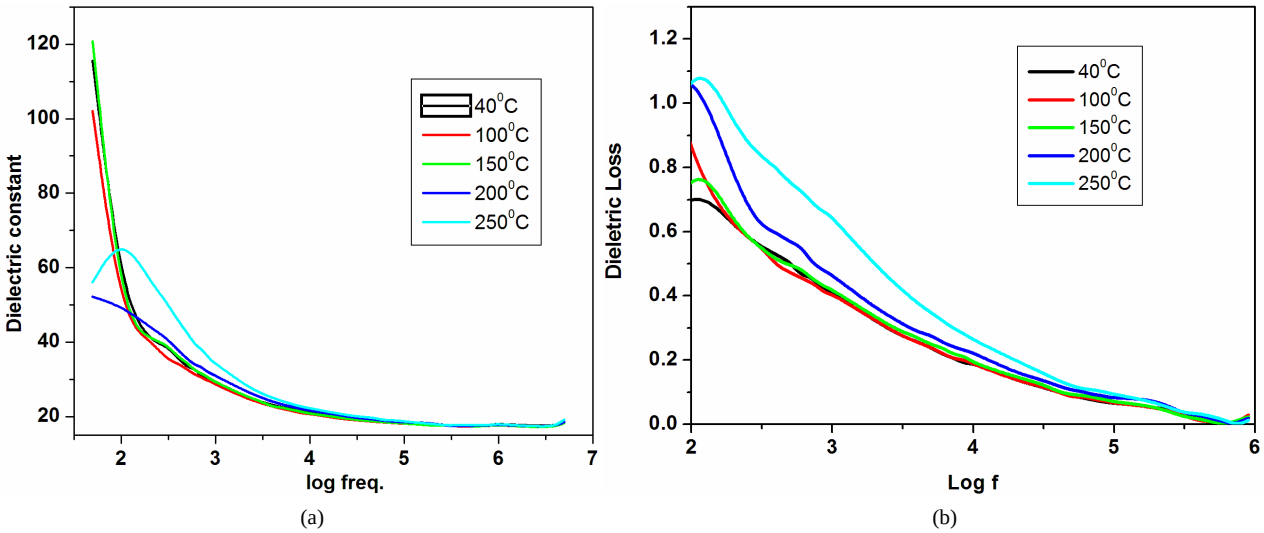

Figure 10. (a) Variation of dielectric constant (ε') with log$f$; (b) Variation of dielectric loss (ε'') with log$f$.

cates very high purity of the material. These curves suggest that the dielectric loss is strongly dependent on the frequency of the applied field.

3.9. Second Harmonic Generation

A high-intensity Nd:YAG laser (λ = 1064 nm) with a pulse duration of 10 ns was passed through the powdered sample of $La_4Mo_7O_{27}$. The SHG behaviour was confirmed by the Kurtz-Perry powder technique [16] from the output of the laser beam having the bright green emission (λ = 532 nm). The second harmonic signal of 1.3 mV for $La_4Mo_7O_{27}$ was obtained for an input energy of 2 mJ/pulse. But the standard KDP gave a SHG signal of 14.5 mv for the same input energy.

4. Conclusion

The single crystal of size 0.8 × 0.3 × 0.2 mm^3 $La_4Mo_7O_{27}$ was grown by high-temperature solution growth technique (flux growth) using H_3BO_3 as flux and was confirmed by X-ray diffraction and FTIR studies. The optical absorbance data gave maximum absorption from 500 - 2000 nm. Its optical band gap values and the refractive index (n) were calculated. The PL studies showed a sharp peak at 2.32 eV. The thermal studies reveal that the compound is stable up to 100˚C and the compound begins to decompose at this temperature. Structural phase transitions occur in the sample and two more endothermic peaks indicate phase transitions at 91.4˚C and 107.2˚C. The low dielectric loss at high frequencies for the given sample indicates very high purity of the material. The SHG behaviour was confirmed by the Kurtz-Perry powder technique. 1.3 mV was obtained as an output for $La_4Mo_7O_{27}$ compared with standard KDP material.

Acknowledgements

Authors are grateful to the Defence Research and Development Organisation (DRDO), Government of India, for funding the project (Sanction order No. ERIP/ER/0703671/M/01/1172 dated. August 24, 2009).

REFERENCES

[1] V. G. Dmitriev, G. G. Gurzadyan and D. N. Nicogosyan, "Handbook of Nonlinear Optical Crystals," Springer-Verlag, New York, 1999. http://dx.doi.org/10.1007/978-3-540-46793-9

[2] D. M. Burland, R. D. Miller and C. A. Walsh, "Second-Order Nonlinearity in Poled-Polymer Systems," *Chemical Reviews*, Vol. 94, No. 1, 1994, pp. 31-75. http://dx.doi.org/10.1021/cr00025a002

[3] C. Chen and G. Liu, "Recent Advances in Nonlinear Optical and Electro-Optical Materials," *Annual Review of Materials Science*, Vol. 16, 1986, pp. 203-243. http://dx.doi.org/10.1146/annurev.ms.16.080186.001223

[4] T. Sasaki, Y. Mori, M. Yoshimura, Y. Yap and T. Kamimura, "Recent Development of Nonlinear Optical Borate Crystals: Key Materials for Generation of Visible and UV Light," *Materials Science and Engineering*: *R*, Vol. 30, No. 1-2, 2000, pp. 1-54.

[5] H. Naruke and T. Yamase, "Crystallization and Structural Characterization of Two Europium Molybdates, $Eu_4Mo_7O_{27}$ and $Eu_6Mo_{10}O_{39}$," *Journal of Solid State Chemistry*, Vol. 161, No. 1, 2001, pp. 85-92. http://dx.doi.org/10.1006/jssc.2001.9284

[6] H. Naruke and T. Yamase, "A Novel Phase in the Gd_2O_3-MoO_3 System," *Acta Crystallographica*, Vol. E58, 2002, pp. i62-i64.

[7] B. van der Wolf, P. Held and P. Becker, "The Lanthanum(III) Molybdate(VI) $La_4Mo_7O_{27,}$" *Acta Crystallographica*, Vol. E65, 2009, p. i59.

[8] H. L. Bhat, "Growth and Characterization of Some Novel Crystals for Nonlinear Optical Applications," *Bulletin of Materials Science*, Vol. 17, No. 7, 1994, pp. 1233-1249. http://dx.doi.org/10.1007/BF02747223

[9] N. F. Mott and R. W. Gurney, "Electronic Processes in Ionic Crystals," 2nd Edition, Oxford, London, 1940.

[10] J. Tauc, "Amorphous and Liquid Semiconductors," Plenum, New York, 1974. http://dx.doi.org/10.1007/BF02747223

[11] C. T. Hsieh, J. M. Chen, H. H. Lin and H. C. Shih, "Field Emission from Various CuO Nanostructures," *Applied Physics Letters*, Vol. 83, No. 16, 2003, pp. 3383-3385. http://dx.doi.org/10.1063/1.1619229

[12] P. Zu, Z. K. Tang, G. K. L. Wong, M. Kawasaki, A. Ohtomo, H. Koinuma and Y. Segawa, "Ultraviolet Spontaneous and Stimulated Emissions from ZnO Microcrystallite Thin Films at Room Temperature," *Solid State Communications*, Vol. 103, No. 8, 1997, pp. 459-463. http://dx.doi.org/10.1016/S0038-1098(97)00216-0

[13] X. Goa, X. Li and W. D. Yu, "Rapid Preparation, Characterization and Photoluminescence of ZnO Films by a Novel Chemical Method," *Materials Research Bulletin*, Vol. 40, No. 7, 2005, pp. 1104-1111. http://dx.doi.org/10.1016/S0038-1098(97)00216-0

[14] M. Cusac, "The Electrical and Magnetic Properties of Solids," Longmans, London, 1967.

[15] J. P. Suchet, "Electrical Conduction in Solid Materials," Pergamon, London, 1975.

[16] S. K. Kurtz and T. T. Perry, "A Powder Technique for the Evaluation of Nonlinear Optical Materials," *Journal of Applied Physics*, Vol. 39, No. 8, 1968, pp. 3798-3813. http://dx.doi.org/10.1063/1.1656857